Review

Susmita Das* and Vimal Chandra Srivastava*

An overview of the synthesis of CuO-ZnO nanocomposite for environmental and other applications

https://doi.org/10.1515/ntrev-2017-0144
Received May 15, 2017; accepted November 20, 2017; previously published online April 13, 2018

Abstract: In the field of environmental science, metal oxide nanocomposites have gained a great attention for both theoretical and experimental aspects of their upgradation because of their wide range of practical applications such as catalysts, sensors, hydrogen storages, and optoelectronics. Among all nanocomposites, Copper oxide-zinc oxide (CuO-ZnO) has attracted more research due to their excellent tunable catalytic, electrical, optical, and magnetic properties and environment-friendly nature. Coupling of one metal oxide semiconductor with another metal oxide semiconductor produces an enlarged surface area, which provide more reactive sites, promotes mass transfer, promotes electron transfer, and avoids photocorrosion of nanocomposites, which enhances its efficiency. The CuO-ZnO nanocomposite has been prepared by various methods such as co-precipitation, sol-gel, wet impregnation, and thermal decomposition. Depending on the preparation method and conditions used, different types of CuO-ZnO nanocomposites like Cu-doped ZnO, Cu supported/impregnated on ZnO, and CuO-ZnO mixed oxides with different morphologies of CuO-ZnO nanocomposites have been obtained. This article reviews the synthesis techniques of the CuO-ZnO nanocomposite and its morphology. Various practical applications of the CuO-ZnO nanocomposites have also been discussed.

Keywords: catalyst; Cu-doped ZnO; nanocomposite; semiconductor; sensor.

***Corresponding authors: Susmita Das and Vimal Chandra Srivastava,** Department of Chemical Engineering, Indian Institute of Technology Roorkee, Roorkee-247667, India, e-mail: susmita.82.das@gmail.com (S. Das), vimalcsr@yahoo.co.in, vimalfch@iitr.ac.in. http://orcid.org/0000-0001-5321-7981 (V.C. Srivastava)

1 Introduction

During the past decade, mixed metal oxide semiconductors have gained a great attention from researchers from various fields such as physics, chemistry, and material science due to their various practical applications such as photocatalyst, sensor, microelectronic circuit fabrication, piezoelectric devices, fuel cell, and solar cell [1–6]. Metal oxide semiconductors have several interesting properties such as natural p-n characteristics, broad light absorption, fast dynamic response, and better sensitivity of change in humidity. More importantly, tuning of band gap energy by adding two different materials is a great advantage in the field of nanotechnology. Further, production of nanocomposite with controllable shapes, sizes, and surface properties is important for different practical applications. In this context, researchers have shown great interest in copper oxide-zinc oxide (CuO-ZnO) mixed semiconductors among all other feasible p-n type mixed semiconductors such as $TiO_2 \cdot NiO$ [2], $CuO \cdot SnO_2$ [4], $SnO_2 \cdot NiO$ [5], and $CuO \cdot TiO_2$ [7, 8]. Zn oxide (ZnO) and CuO are n- and p-type semiconductors, respectively, with a band gap of 3.37 eV and 1.2 eV. Their conductivities are in the range 10^{-7}–10^{-3} S/cm for ZnO and 10^{-4} S/cm for CuO [9–13].

Various researchers like Nakamura et al. [14], Ushio et al. [15], Baek and Tuller [16], etc., have synthesized CuO-ZnO heterojunctions and shown their opportunity in various environmental field. Further, several researchers have prepared CuO-ZnO nanocomposites using techniques such as thermal decomposition [1], co-precipitation [17], chemical vapor deposition [18], sol-gel and wet-impregnation methods [19, 20], complex-directed hybridization, and heating brass in air [21]. Literature shows that in comparison to its individual component (pure ZnO or CuO), CuO-ZnO nanocomposites exhibit better results in various practical fields [1, 17, 22–25]. For example, Saravanam et al. [1] and Li and Wang [17] showed a better photocatalytic performance of CuO-ZnO nanocomposites than its individual component (pure CuO or ZnO). Zhao et al. [22] and Wang et al. [23] showed a better gas-sensing

ability of Cu-doped ZnO nanocomposites than pure ZnO. Karunakaran and Manikandan [24] showed the nanocomposite as a better supercapacitor than pure CuO.

In this context, there are reviews present in the literature in the field of nanocomposites [26–30], whereas reviews on metal nanocomposites, specifically Cu dopant ZnO nanocomposites, have not been reported yet. The aim of this article is to help researchers that are involved in the field of metal nanocomposites by compiling the data on various synthesis methods, morphology of CuO-ZnO nanocomposites, and importantly its various applications in the field of catalyst, solar cell, sensor, and optoelectronics devices.

2 Synthesis of CuO-ZnO nanocomposite

It is essential to differentiate between Cu-doped ZnO, Cu supported/impregnated on ZnO, and CuO-ZnO mixed oxides. In the literature, depending upon the size of the catalysts, they are also referred to as CuO-ZnO nanocomposites. Cu-doped ZnO is the catalysts in which the atoms of Cu get inserted to take the place of Zn in the crystal lattice of the ZnO. In this type of catalyst, XRD analysis only gives the peaks of ZnO; however, crystal parameters get altered because of the Cu doping. EDX and other elemental analysis techniques give the presence of Cu. It may be noted that in the Cu-doped ZnO, atomic (at.) % of Cu is very less. Zhao et al. [22] has reported that the Cu-doped ZnO nanofibers prepared by electrospinning technology can have a maximum of 6 at.%. Tiwari et al. [31] prepared Cu-doped 5 at.% ZnO ($Zn_{0.95}Cu_{0.05}O$) films grown on c-plane sapphire substrates prepared by pulsed laser deposition technique. Liu et al. [32] reported that a second phase appears when the Cu-doping concentration in ZnO is greater than 5 at.%. At higher Cu at.%, peaks corresponding to Cu phases start to appear in the XRD spectra. Similarly, in Raman spectroscopy of Cu-doped ZnO, the intensity of the E_{1L} mode (related to oxygen vacancy and Zn interstitial defects in ZnO) increases when compared with the corresponding peak in pure ZnO [22, 33]. A broad band at 540–670 cm^{-1} in the Raman spectra of Cu-doped ZnO indicates intrinsic lattice defects and often arises by the doping [34]. Also, the E_{2H} mode of Cu-doped ZnO nanofibers gets shifted to a higher frequency because of the distortion of the lattice and the defects due to doping of Cu in the ZnO lattice [35, 36].

Cu supported/impregnated on ZnO has higher Cu at.% and can be prepared by a number of methods such as impregnation, sol-gel, co-precipitation, deposition-precipitation, etc. In the "incipient wetness" or "dry" impregnation method, ZnO suspension is treated with a solution of Cu such that the pore volume of ZnO is greater than that of the Cu precursor solution. In the "wet", "soaking", or "diffusion" impregnation, an excess of Cu precursor solution with respect to the pore volume of the support is used. In the sol-gel method, Cu supported on ZnO can be prepared from a homogeneous solution of Zn salts in combination with Cu salts to precipitate the mixed hydroxide, which can be subsequently calcined to obtain the catalysts. After loading of Cu, the resulting material is activated by heating or in combination with other treatments to convert Cu to a more active state. The XRD spectra in the Cu-supported catalysts show presence of both CuO and ZnO phases.

In the mixed oxide, the at.% of Cu and Zn are similar. Again, the phases of both CuO and ZnO are observed in the XRD analysis. In addition to CuO and ZnO, the mixed oxides contain some compounds that have both Cu and Zn elements. In the following section, recent progress in synthesizing high-quality CuO-ZnO composites are discussed.

2.1 Co-precipitation method

Li and Wang [17] prepared hierarchical three-dimensional (3D) morphology CuO-ZnO nanocomposites by a simple one-step homogeneous co-precipitation method. A solution of Zn chloride ($ZnCl_2$) and Cu sulfate ($CuSO_4 \cdot 5H_2O$) was kept within a sealed bottle for 24 h at 80°C. The precipitate was centrifuged and dried to obtain a final powder product. The nanocomposite was composed of flowerlike ZnO microstructures adorned with leaf-like CuO nanopatches. In a similar manner, Das and Srivastava [37] also prepared hierarchical 3D morphology CuO-ZnO nanocomposites where Cu (II) chloride and Zn sulfate were used as precursors, and other experimental conditions were kept similar. The results showed the nanocomposite as a mixture of flower-shaped ZnO (with a diameter of about 1–2 μm) and leaf-shaped CuO (Figure 1). Gajendiran and Rajendran [13] fabricated aggregated spherical morphology CuO-ZnO nanocomposites in the size range of 10–35 nm using a co-precipitation method. Zn acetate dehydrate and Cu acetate dehydrate were used as precursors. Three different kinds of solvents such as water, water/monohydric alcohol (ethanol), and water/dihydric alcohol (ethane-1,2-diol) were used for experimental purposes. It has been shown that using a different solvent, the system viscosity and surface tension could be changed, which, in turn, could control the nucleation, crystal orientation,

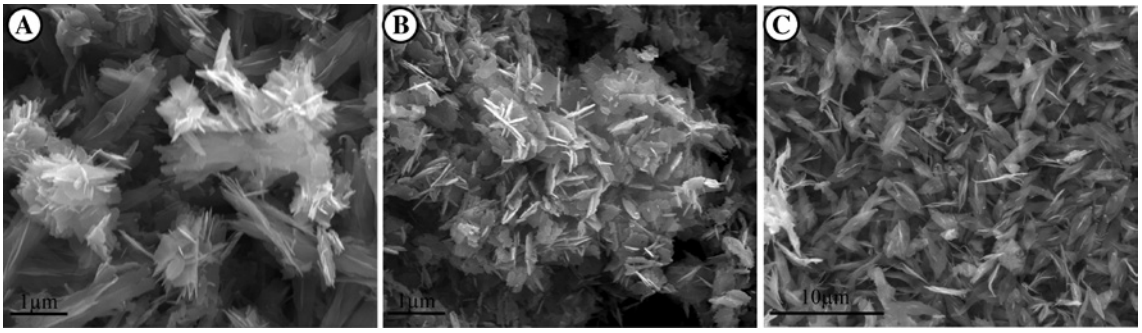

Figure 1: SEM image of (A) CuO-ZnO nanocomposite, (B) Zn oxide nanoparticles, (C) Cu oxide nanoparticles. Copyrights reserved to the Material Science Forum [37].

crystal size, and crystal growth. Bagabas et al. [38] synthesized CuO-doped ZnO nanocomposites using cyclohexalamine by the co-precipitation method. For experimental purposes a different percentage of CuO was loaded with the ZnO nanoparticle. Liu et al. [39] prepared spherical nanocomposites by coordination oxidation homogeneous co-precipitation method where pure Cu metal and ZnO were used as precursors.

2.2 Chemical vapor deposition

Simon et al. [18] fabricated 1D ~400-nm-long nanorod-shaped CuO-ZnO nanocomposites on Si(100) substrates in two steps. First, the plasma-enhanced chemical vapor deposition (PE-CVD) method was used for the depositing ZnO nanorod (NR) arrays on silicon substrate. Thereafter, CuO was dispersed over ZnO followed by thermal treatment in air. Experiments were carried out for various CuO loadings (variation of RF power) on ZnO nanorods to analyze the effect on the performance of hydrogen production rate.

2.3 Sol-gel method

Different researchers have prepared CuO-ZnO nanocomposites by the sol-gel technique using different precursors. Vijayakumar et al. [19] prepared cylindrical CuO-ZnO nanofibers with a diameter (d) ~50–100 nm by the sol-gel method as shown in Figure 2. A clear viscous solution of poly(vinyl alcohol)/Zn acetate/Cu acetate composite sol was prepared by adding a precursor into deionized water. Subsequently, the electrospinning method was used to prepare the final CuO-ZnO nanocomposite using the above-prepared composite sol solution. To obtain the final product, the resultant PVA/Zn acetate/Cu acetate composite fibers were calcined at 600°C in air. Haque et al. [40] synthesized flower-shaped ~21-nm CuO-ZnO nanocomposites, where Zn acetate dehydrate and Cu acetate were used as precursors. Gomez-Pozos et al. [41] prepared a Cu-doped ZnO thin film using Zn acetate and two Cu precursors such as Cu acetate and Cu chloride. Udayabhaskar and Karthikeyan [42] synthesized agglomerated flake-like morphology nanocomposites, where Zn nitrate and Cu nitrate were used as precursors for experimental

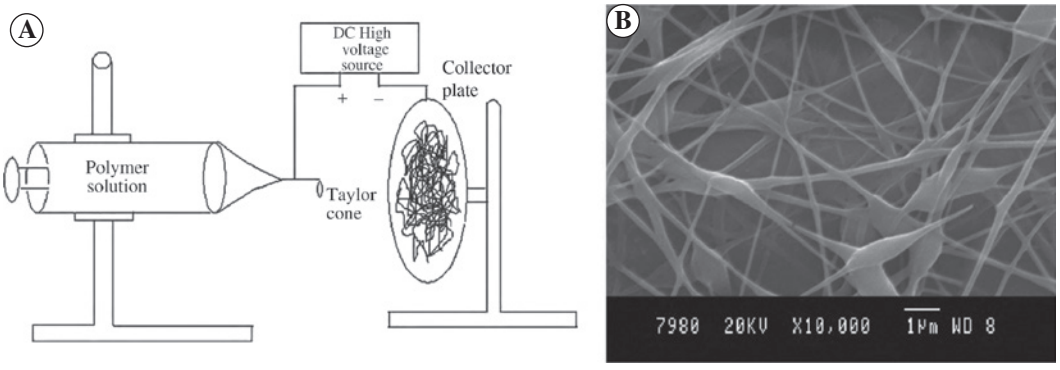

Figure 2: (A) Production of CuO-ZnO nanocomposite by sol-gel and electrospinning methods. (B) SEM image of CuO-ZnO nanocomposite. Copyrights reserved to Elsevier [19].

purposes. Liu et al. [43] also synthesized hexagonal CuO-ZnO nanorods using the same precursors of Cu nitrate and Zn nitrate. Muzakki et al. [44] synthesized monoclinic CuO-doped hexagonal wurtzite ZnO-shaped CuO-ZnO nanocomposites, where Zn sulfate heptahydrate and Cu sulfate pentahydrate were used as precursors for experimental purposes.

2.4 Wet impregnation method

Sathishkumar et al. [20] synthesized CuO-ZnO nanofibers by the wet impregnation method. ZnO nanoparticles were mixed with an aqueous solution of Cu sulfate $CuSO_4 \cdot 5H_2O$ with stirring for 48 h for the incorporation of CuO on ZnO. The mixture was heated at 100°C for 24 h to evaporate the unwanted water and calcinated at 550°C for 5 h. In the final product, the CuO nanoparticles (20–30 nm) were attached to truncated octahedron or cuboctahedron-shaped ZnO edges.

2.5 Thermal decomposition method

Saravanan et al. [1] synthesized CuO-ZnO nanocomposites of different weight ratios by a simple cost-effective thermal decomposition method. Ground Zn acetate dehydrate and Cu acetate mixture were annealed at 350°C for 3 h to obtain the CuO-ZnO nanocomposite. The percentages of Cu acetate were varied to produce different wt% CuO-loaded ZnO nanocomposites. CuO-ZnO was in a rod-shaped morphology with a diameter of ~35 nm. The lengths (L) of the nanorods varied from 50–500 nm by varying the wt% of the CuO loading.

2.6 The complex-directed hybridization

Yang et al. [21] prepared CuO-ZnO hybrid nanostructures by complex-directed hybridization and subsequent calcination method. A solution of Zn acetate was mixed with Cu nitrate solution under vigorous stirring at a particular temperature and kept for 10 min. Further, the solution was heated under reflux for another 50 min at the same temperature. Finally, the dried products were annealed at 350°C for 2.5 h.

2.7 Directly heating brass in air

Zhu et al. [45] fabricated CuO-ZnO nanocomposites (binary oxide) by direct heating of CuZn alloy (brass) on a hotplate for 2 days. The concentration of Zn was varied within 5–40 wt% and the temperature within 350°C–540°C in order to synthesize a different morphology such as a nanowire (Zn 5 wt%) of length ~6–8 μm, diameter of ~40–60 nm, nanoflakes (Zn 49 wt%) of length ~4 μm with a very sharp tip with a diameter of ~10–20 nm, etc.

2.8 Electrospinning

Zhou et al. [46] synthesized 3D porous CuO-ZnO hierarchical nanocomposites by the co-electrospinning process. A solution of Zn acetate with two crystals of water was prepared by adding a mixed solvent of N,N-dimethylformamide and ethanol. Finally, a sol solution was prepared by adding poly(vinyl pyrrolidone) (PVP) with the above-mentioned prepared solution under vigorous stirring for 5 h. Similarly, another solution of Cu acetate with one crystal of water was prepared by adding a mixed solvent of DMF, ethanol, and acetic acid under stirring. The final sol solution was prepared by adding PVP to the above-mentioned mixture under vigorous stirring for 12 h. A sol solution of Zn acetate and Cu acetate were used as the outer and inner solutions, respectively, during the experiment. After carrying out the experiment in a co-electrospinner, the obtained precursor fibers were annealed with a rising rate of 1°C/min to 500°C and kept for 3 h, forming the CuO-ZnO HNCs. The obtained randomly oriented CuO-ZnO nanocomposites were in a truncated wire shape with a diameter of ~200 nm, which was also composed of small CuO nanoparticles with a diameter of ~20 nm at the outer surface of the nanowires. Ang et al. [47] synthesized CuO-ZnO nanocomposite film indium tin oxide (ITO)-coated glass slides by the cathodic co-electrodeposition route. Zn nitrate and Cu acetate were used as the precursor solution. Experiments were carried out for different Cu loadings. The results showed that depending on Cu loading, the flower-shaped ZnO changed to flowerlike superstructures with assemblies of flakes and grains. Zhao et al. [22] synthesized ~100-nm diameter of Cu-doped ZnO nanofibers (length approximately several millimeters) by electrospinning technology. The nanofiber surfaces were composed of nanoparticles with diameters around 20–50 nm. A sol solution of Cu chloride and Zn acetate were prepared by adding an aqueous solution of polyvinyl alcohol. Composite fibers were prepared using the above-mentioned prepared sol solution with the help of an electrospinning apparatus. Finally, the obtained composite fibers were heated at 650°C for 3 h to synthesize the final product. Various amounts of CuO were used to produce different % loadings of ZnO. Jeong et al. [48]

also prepared ZnO · Cu_2O heterojunction films by consecutive cathodic electrodeposition of ZnO and Cu_2O on glass plates covered with a SnO_2:F transparent conductive oxide layer (Asahi glass). First, an aqueous solution of Zn nitrate was used in fabricating the ZnO layer on the SnO_2 conductive glass substrates. Further, the Cu_2O layer was deposited on the ZnO layer using an aqueous Cu sulfate solution.

2.9 Thermal oxidation

Zhao et al. [49] prepared CuO-ZnO nanocomposites by the thermal oxidation method. Two pure Cu and Zn sheets were closely packed together and kept in a resistively heated furnace at 500°C for 4 h to obtain p-CuO and n-ZnO nanowires on the surfaces of two sheets. The heterojunctions were formed between the p-CuO and n-ZnO nanowire interfaces (Figure 3). CuO nanowires and ZnO nanowires were composed together like a compact sheet. Nanorods with widths of 30–100 nm and average lengths of 5–20 µm were obtained. Kargar et al. [50] also prepared CuO-ZnO heterojunction branched nanowires by thermal oxidation and thermal growth method. Initially by the annealing process, CuO nanowires were grown on Cu foils by keeping Cu foils into an open furnace at different temperatures. The obtained CuO nanowires were transferred into a sputtering machine for producing ZnO nanowires on CuO nanowires.

2.10 Microwave synthesis

Vijayalakshmi and Karthick [51] synthesized flower-shaped agglomeration of CuO-ZnO nanocomposites by the microwave synthesis technique. Aqueous NaOH solution was added dropwise to the mixture of an aqueous solution of Zn acetate and Cu acetate, which was kept on a magnetic hot plate at 70°C under stirring. The resultant solution was kept in a microwave at 450 W for 15 min. The obtained white colored product was dried at room temperature after washing several times with absolute ethanol and distilled water. Finally, the product was calcined at 800°C for 7 h. Aliyu et al. [52] also synthesized rod-shaped CuO-ZnO nanocomposites (<70 nm) by the microwave synthesis technique. Aqueous EDTA solution was added dropwise within separately prepared aqueous solution of Zn acetate dehydrate and Cu (II) nitrate under stirring. Both solutions were kept within a Teflon reaction vessel under a microwave oven for 10 min at 90°C and 240 W. Finally, the formed deep blue crystals were washed with absolute ethanol and deionized water, after separating by microfiltration. Ashok et al. [53] also synthesized ~28- and ~34-nm CuO-ZnO nanocomposites by the microwave-assisted technique using ionic liquid. Zn acetate, Cu acetate, 1-butyl-3-methyl imidazolium tetrafluoro borate, and sodium hydroxide were used as the precursor materials for CuO-ZnO nanocomposite preparation.

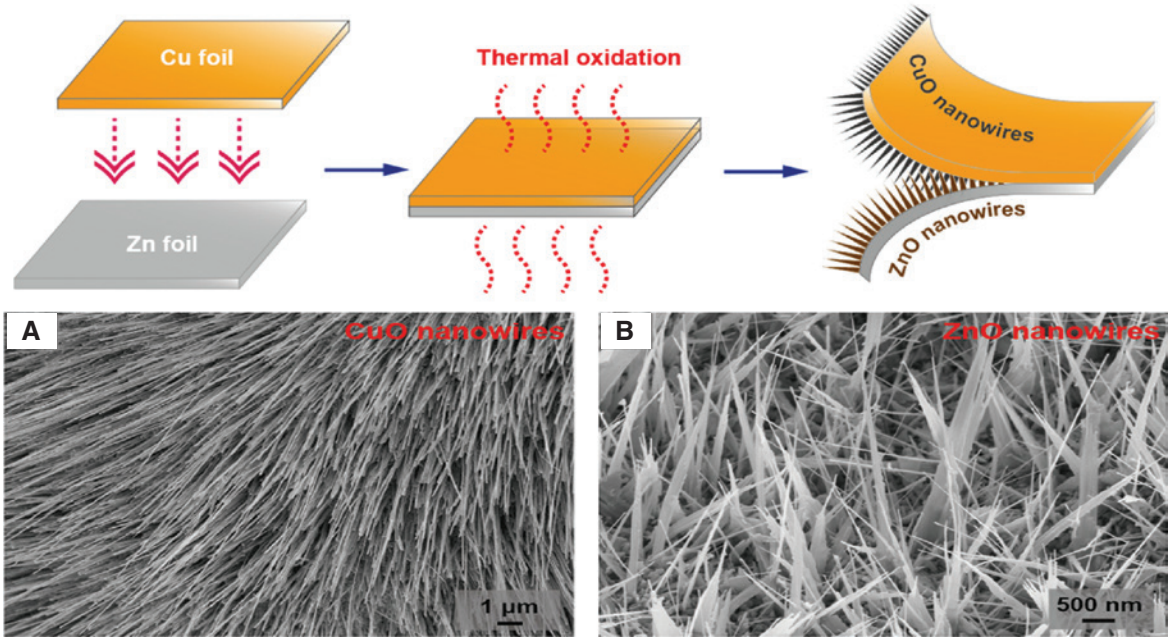

Figure 3: Production of CuO-ZnO nanocomposite by thermal oxidation method. SEM micrograph of (A) p-CuO nanowires and (B) p-ZnO nanowires. Copyrights reserved to Elsevier [49].

2.11 Hydrothermal method

Choudhary et al. [54] synthesized CuO-ZnO nanocomposites on a porous 3D nickel substrate by the stepwise hydrothermal method. The flower-shaped p-typed CuO nanoflakes (in the form of a flower) were successfully grown on the tips of n-type ZnO hexagonal rods. Zn acetate and Cu nitrate were used as precursor solutions for the experiments. Chang et al. [55] prepared nanoplate-shaped CuO-ZnO nanocomposites by the two-step hydrothermal method. Pure ZnO was prepared by autoclaving Zn chloride solution at 120°C for 10 h within a Teflon-lined autoclave. The prepared ZnO nanoplates were added with Cu acetate solution, which was further hydrothermally reacted at 120°C for 8 h to obtain the CuO-ZnO nanocomposites. Zainelabudin et al. [56] prepared CuO-ZnO nanocorals using the low-temperature hydrothermal method. Initially, the ZnO nanorods were grown on an indium tin oxide substrate by immersing the ZnO nanoparticle seed solution-coated tin oxide substrate into a Zn nitrate precursor solution and kept in an oven at 50°C for 6–8 h. The prepared ZnO nanorod substrates were immersed in a Cu nitrate solution at 60°C for 1.5–4 h to grow the CuO nanocoral on the ZnO nanorods. Kim et al. [57] fabricated a CuO-ZnO heterostructure nanorod. The ZnO nanorod was prepared using the hydrothermal method, where a Zn chloride solution was hydrothermally treated in a Teflon autoclave at 150°C for 4 h. The obtained ZnO nanorod was mixed with a Cu nitrate solution and UV-irradiated for 5 min to ~2 h to grow CuO on the ZnO nanorod. Various Cu ion concentration solutions have been used for experimental purposes. Wang et al. [23] fabricated CuO-ZnO nanowires using the modified hydrothermal method, where a solution of Zn chloride and Cu chloride were kept within an autoclave with a screwed small hole at 90°C for 8 h. Karunakaran and Manikandan [24] prepared CuO-ZnO nanocomposites using PVP as a templating agent. Haque et al. [40] prepared nanoflower-structured CuO-ZnO nanocomposites. CuO-ZnO nanocomposite seed was prepared using Zn nitrate and Cu nitrate solution with tetraethylammonium bromide (TEAB) as the surfactant. After further processing, the samples were calcinated at 500°C for 2 h. Datta et al. [58] fabricated a CuO-ZnO nanowire using ZnO nanoparticles as the seed layer. The solution containing the ZnO nanoparticle was spin coated on a Si substrate and then hydrothermally treated for the growth of ZnO nanowires. A thin layer of Cu was deposited on the above-mentioned prepared substrate and thermally oxidized at 400°C for 1 h for the formation of CuO on ZnO nanowires. Zhang et al. [59] hydrothermally prepared CuO-ZnO nanocomposite hollow spheres (~20 nm diameter) using colloidal carbon spheres as templates. A solution of Zn acetate, Cu chloride, and glucose was kept in a Teflon sealed autoclave at 180°C for 24 h. Finally, precipitate was collected and calcined at 500°C for 4 h. Ang et al. [47] also prepared CuO-ZnO corn-like nanocomposites by photochemical deposition of CuO on hydrothermally prepared ZnO nanorod on a glass substrate. Zn acetate, Zn chloride, and Cu nitrate were used as precursors. Xu et al. [60] hydrothermally prepared CuO-ZnO micro/nanoporous array films where various compositions of Cu and Zn were varied for experimental purposes.

2.12 Other methods

There are several other techniques that have also been reported in literature for the synthesis of CuO-ZnO nanocomposites. For example, Sheini et al. [61] prepared Cu · ZnO nanocomposite films by the cathodic electrodeposition method. Experiments were performed within a conventional three-electrode electro-chemical cell using Zn chloride, Cu chloride, and hydrogen peroxide solution as an electrolyte. A polycrystalline Zn foil, a platinum sheet, and a saturated calomel electrode were used as working, counter, and reference electrodes, respectively.

Wang et al. [62] synthesized CuO (tetrapod) · ZnO (whisker) nanocomposites using a simple photo-deposition method. Using the equilibrium gas-controlling method, ZnO nanoparticles were prepared where metallic Zn was used as the main raw material. Prepared ZnO was mixed with a solution of Cu nitrate and PEG water under stirring. Subsequently, sodium hydroxide was added to the solution and irradiated by UV light (254 nm) under stirring at 50°C for 4 h. Precipitate was collected and dried under a vacuum oven at 50°C for 8 h. Xia et al. [63] prepared cluster-like nano/micro CuO-ZnO particles (~200–300 nm) on a brass surface using a dielectric barrier discharge reactor. Soejima et al. [64] synthesized CuO nanoflower/ZnO nanorod composite arrays using a very easy alkaline vapor oxidation method as shown in Figure 4. A brass plate was immersed in an aqueous NH_3 solution for various time durations in a drying oven at 80°C. Das and Srivastava [65] prepared spherical CuO-ZnO nanocomposites by the electrochemical method where aqueous succinic acid was used as an electrolyte solution. Cu and Zn electrodes were used as anodes, whereas only the Zn electrode was used as a cathode. Several other researchers like Wang and Lin [11], Buchholz and Chang [66], Jacob et al. [67], Minami et al. [68], and Jiang et al. [69] also prepared CuO-ZnO nanocomposites by a two-step solution process, pulsed-laser ablation, solid state metathesis technique, and electrodeposition method, respectively.

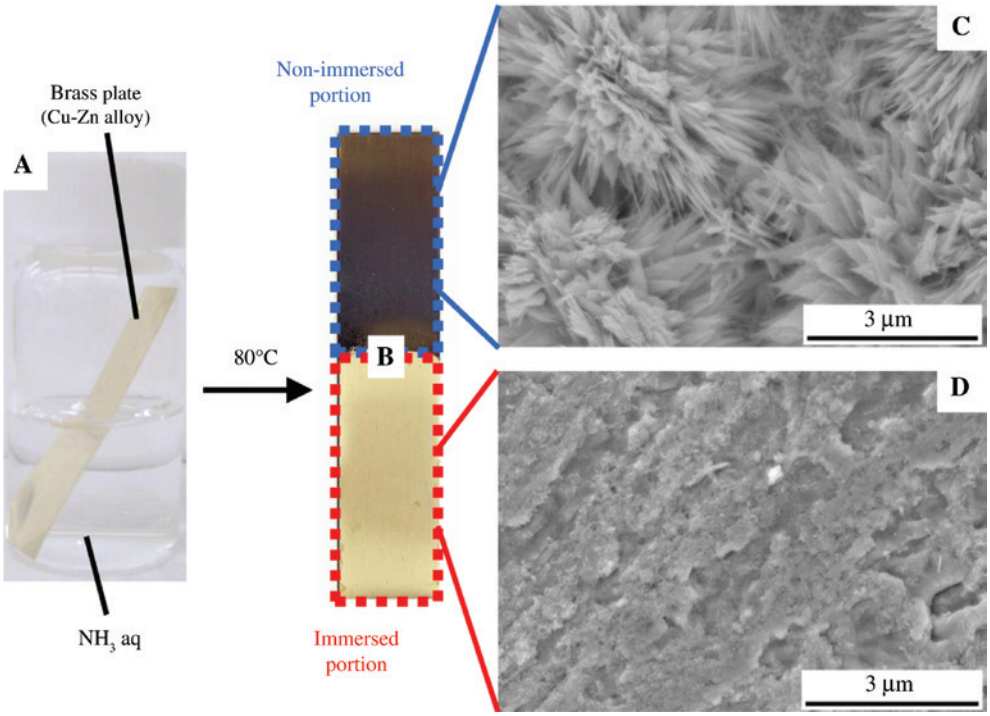

Figure 4: Production of CuO-ZnO nanocomposite by an alkaline vapor oxidation process. SEM images of brass plate at the non-immersed portion (C) and the immersed portion (D) after the reaction. Copyrights reserved to Elsevier [64].

3 Influence of CuO introduction in the ZnO nanostructures on various properties

The final structure of the material greatly depends on the synthesis methods. For the same composition of Cu and Zn in the composite, the method of preparation has tremendous effect on the structure as well as on the properties. The CuO-ZnO nanocomposites are of different shapes such as spherical, cylindrical, rod shaped, nanowires, flowerlike, nanofilms, nanoflakes, etc. The morphology, structure, and properties of the CuO-ZnO nanocomposites have been found to vary with the composition.

The ZnO particles generally possess a polycrystalline hexagonal wurtzite structure. The Cu-supported ZnO nanoparticles show minor peaks assigned to the CuO monoclinic phase. The XRD peaks shift slightly toward lower values indicating that the Cu atoms have replaced the Zn atoms in the Cu-doped ZnO. Literature shows that only samples with Cu content lower than 15% are one-phase wurtzite-like $Cu_xZn_{1-x}O$, while those with higher Cu content include a tenorite-like oxide ($Zn_xCu_{1-x}O$) phase [70, 71]. Cu atoms replace Zn in the hexagonal lattice, and/or Cu segregate to the noncrystalline region in the grain boundary [72]. In the Cu-doped ZnO samples, the Fourier-transform infrared spectroscopy (FTIR) shows the absorption band near 620 cm^{-1}, which is related to the vibration of the Cu–O bond [73]. Lighter metal (like Mg)-doped ZnO shows a shift in the stretching bond position of Zn–O toward the higher wave numbers [74]. However, Zn and Cu have similar masses (63.5 amu for Cu and 65.4 amu for Zn). Therefore, this shift is not recognizable in Cu-doped particles [71].

The dopant (Cu) incorporation into ZnO decreases its band gap. This is due to the fact that the 3d orbital of the Cu atom is much shallow than the 3d orbital of Zn. Therefore, strong coupling occurs between the d orbital of the Cu atom and the p orbital of the O atom, which narrows the direct band gap. Also, the Cu 3d orbital creates impurity bands above the ZnO valance band, which further helps in decreasing the band gap [71, 75]. Pure and doped ZnO nanofluids showed good antibacterial activity, which increases with Cu doping [71].

The Cu oxidative state plays an important role in different applications. Therefore, the determination of the Cu valence in a CuO-ZnO composite is very important. The possible ionic states of Cu as a dopant are Cu^+ and Cu^{2+}, and their corresponding ionic radii are 96 pm and 72 pm, respectively [36, 76]. The ionic radius of Zn^{2+} in the hexagonal wurtzite ZnO is 74 pm. During the synthesis of Cu-doped ZnO, the dopant Cu has the possibilities of substituting Zn ions in the lattice site or may occupy the

interstitial position and form impurity phases [42]. The shift in the (101) plane's XRD peak to the higher angle side usually arises by the substitution of the Zn ions with the dopant ion of the lower ionic radius, i.e. by Cu^{2+} instead of Cu^{+}. This shift is usually very low because of the similar ionic radii values of Zn^{2+} and Cu^{2+} [77]. This substitution also causes reduction in lattice parameters and shrinkage in the unit [23, 42, 62, 78].

Surface doping of ZnO with Cu and the valence of Cu in the CuO-ZnO nanocomposites can be studied using X-ray photoelectron spectroscopy (XPS). The XPS spectra of Cu-doped ZnO show peaks at ~930 and ~950 eV corresponding to the atomic term symbols $2P_{3/2}$ and $2P_{1/2}$ of Cu^{2+} [69]. The chemical shifts observed are consistent with Cu–O binding. If spectral shoulders are observed at ~940 and 960 eV, it means that Cu exists in a mixed valence state [79]. Hence, on the ZnO surface, Cu exists as nonstoichiometric cupric oxide ($Cu^{1+\delta O}$) [67, 79, 80].

Experimental determination of the magnetic moment can also help in determining the valence of Cu in the CuO-ZnO nanocomposite. An outer cell electronic configuration of Cu atoms in the unionized state is $3d^{10}4s^{1}$. Thus, Cu^{+} and Cu^{2+} ions have an electronic configuration of $3d^{10}$ and $3d^{9}$, respectively. In the $3d^{10}$ configuration, all the d electrons are paired, and hence, Cu^{+} ions do not posses any magnetic moment. For the Cu^{2+} ions, one unpaired electron is available, which gives rise to a spin angular momentum of ½. This results in a net magnetic moment of $M = [\mu_B \{S(S+1)\}^{0.5}$; $g = 2$, $S = 1/2] \approx 1.73\ \mu_B$ [31, 81]. If the experimentally determined magnetic moment is similar to the theoretical magnetic moment value for Cu^{2+} ions, it shows a presence of Cu ion in the predominant Cu^{2+} state [31]. Thus, the experimentally determined magnetic moment of the CuO-ZnO nanocomposites gives an insight into the possible valence of Cu ions in the material.

4 Various applications of CuO-ZnO nanocomposites

4.1 Photocatalytic degradation of pollutant

Several researchers have utilized CuO-ZnO nanocomposites for the photocatalytic degradation of different dyes, for example, the methylene orange dye degradation efficiency (η) of ~88–93% within 120 min of UV irradiation [1, 61]. Ang et al. [47] reported a methyl orange degradation efficiency of ~90% after 90 min under UV irradiation as shown in Table 1. Chang et al. [55] showed a 100% degradation efficiency within 40 min under UV irradiation. Liu et al. [32] reported a degradation efficiency of methyl orange (~90%) with variation in the calcination temperature of nanocomposites. Zhang et al. [59] showed that, compared to commercially available TiO_2 or pure ZnO nanoparticle, CuO-ZnO hollow spherical nanocomposites display a better photocatalytic efficiency ~98% for methylene blue degradation within 60 min of UV irradiation. Saravanan et al. [1], Muzakki et al. [44] and Das and Srivastava [37] reported ~97%, 94%, and ~100% methylene blue dye degradation efficiency at 120, 120, and 30 min of UV irradiation, respectively. Sathishkumar et al. [20] reported a photocatalytic activity of CuO-ZnO nanocomposites to be two times more than bare ZnO for acid red 88 degradation. Jung and Yong [82] showed an effective degradation efficiency of CuO-ZnO nanocomposites formed

Table 1: Photocatalytic application of CuO-ZnO nanocomposite for different toxic dyes.

Toxic dye	η for CuO-ZnO (%)	η for ZnO (%)	Light source and time (min)	References
Methylene blue, methyl orange	97.2, 87.7	0.9, 3.1	UV, 120 min	Saravanan et al. [1]
Methylene blue, methyl orange	100, 100	30, 35	UV, 25 min	Chang et al. [55]
Methylene blue	90	55	UV, 90 min	Zhang et al. [59]
Methylene blue	94	10	UV, 120 min	Muzakki et al. [44]
Methylene blue	97	75	UV, 30 min	Das and Srivastava [37]
Methyl orange	93	65	UV, 120 min	Wang et al. [62]
Methyl orange	65, 90	20, 20	UV and sunlight, 150 min	Ang et al. [47]
Methyl orange	88	50	UV, 60 min	Liu et al. [32]
Methyl orange	90	50	UV, 60 min	Liu et al. [32]
Methyl orange	90	-	UV, 120 min	Zhang [10]
Acid red 88	100	20	UV, 60 min	Sathishkumar et al. [20]
Acid orange 7	90	60	UV, 240 min	Jung and Yong [82]
Rhodamine B	100	37	UV, 120 min	Li and Wang [17]
Rhodamine B	100	40	UV, 60 min	Liu et al. [83]
Rhodamine B	40	–	UV, 325 min	Yang et al. [21]

Table 2: Photovoltaic properties of CuO-ZnO nanocomposite as solar cell.

Short-circuit photocurrent density (J_{sc}) mA/cm^2	Open circuit voltage (V_{oc}) (V)	Fill factor (FF)	Conversion efficiency (η) (%)	References
1.6	2.8×10^{-4}	0.25	1.1×10^{-4}	Kidowaki et al. [88]
2.69	316×10^{-3}	48	0.41	Jeong et al. [48]
6.94	0.41	0.53	1.52	Minami et al. [69]
2.34	0.13	0.29	0.1	Hsueh et al. [89]

on a stainless steel substrate for the acid orange 7 dye. Li and Wang [17] showed that a comparative results of photocatalytic degradation efficiency by pure ZnO, CuO, and CuO-ZnO nanocomposites were 37%, 56%, and ~100%, respectively, for rhodamine B dye under simulated sunlight at 2 h. Liu et al. [84] reported an ~90% photocalatytic degradation efficiency of rhodamine B at 2 h under UV irradiation. Yang et al. [21] reported an ~38% rhodamine B degradation efficiency within 330 min under UV irradiation. Jacob et al. [67] showed an improved photocatalytic degradation efficiency of both anodic dye and cathodic dye using nanocomposites. Bagabas et al. [38] revealed that the CuO-ZnO nanocomposite could photocatalytically degrade cyanide. The results show that with an increase in CuO dopant from 1 to 4 wt%, the degradation efficiency increased from 56% to 97%.

Overall, the above-mentioned results illustrate a better degradation efficiency of a nanocomposite than its individual components. The probable reason behind the enhanced photocatalytic activity of a nanocomposite is because of the structural effects such as a large specific surface area and a porous structure of ZnO, which enhance the mass transfer and diffusivity of the dye molecules and oxygen species. Furthermore, under photo irradiation, the nanocomposite work as a p-n junction, which reduces the recombination rate and aid in the split-up of electron hole pairs, and consequently, active hydroxyl radicals get produced in higher quantities [28].

4.2 Gas sensor

Pure ZnO is a very good gas sensor device, but the working temperature of ZnO is higher than other gas-sensing materials such as SnO_2 [85–87]. The reactive surface of a semiconductor material plays an important role in the catalytic oxidation of a gas molecule, which indirectly detects gases. Researchers have tried to solve the above-mentioned problem by incorporating CuO within ZnO, and it was shown that the CuO-ZnO nanocomposite could be a very good gas sensor. For example, Yang et al. [21] used the synthesized CuO-ZnO hybrids as a p-type sensor in response to reducing gases such as acetone, ethanol, and xylene. The response of the CuO-ZnO sensor was maximum for acetone, ~2.8, and the response of other gases such as ethanol, xylene, methanol, 4-cyclohexene, 4-toluene, benzene, and cyclohexane was 2.5, 2.4, 2.4, 2.1, 1.7, 1.3, and 1.3, respectively, for 200 ppm of the sample at 240°C. Wang et al. [23] analyzed the gas-sensing capability of the nanocomposite for carbon monoxide gas, and the response was found to be 7.6 at 300°C for 300 ppm CO. Kim et al. [57] reported an enhanced H_2S gas-sensing capability of the nanocomposite at a sensing temperature ≤500°C than the pure ZnO nanorod. The sensing response was 890 for 50 ppm H_2S. Xu et al. [60] also showed the application of the CuO-ZnO nanocomposite as a good H_2S gas (10 ppm) sensor. Furthermore, Xia et al. [63] showed the application of the nanocomposite for cataluminescence sensing (CL intensity counting ~400) of acetic acid. Gomez-Pozos et al. [41] showed the nanocomposite application as a propane gas sensor, for 500 ppm at 300°C working temperature. Huang et al. [87] showed an improved gas-sensing capability of the nanocomposite than for pure ZnO for a volatile organic compound. The response of ZnO (320°C) and the CuO-ZnO (220°C) sensor for 100 ppm ethanol, formaldehyde, and hydrogen sulfide was found to be 25.5, 28.9, and 25; and 22, 12, and 5, respectively. Overall, the results show that the gas-sensing response of the nanocomposite is much higher that of pure ZnO. The above result is due to the 3D hierarchical morphology of the CuO-ZnO morphology, which provides large active sites (large surface to volume ratio) with higher porosity, which enhances the catalytic reaction, gas diffusion, and mass transportation in gas-sensing materials.

4.3 Solar cell

Few researchers showed the application of the CuO-ZnO nanocomposite as a solar cell. Kidowaki et al. [88], Jeong et al. [48], Minami et al. [68], and Hsueh et al. [89] showed that the conversion efficiency of the nanocomposite solar cell was 1.1×10^{-4}%, 0.41%, 1.52% and 0.1%, respectively. All other photovoltaic properties are listed in Table 2.

4.4 Hydrogen generation

Several researchers showed the application of CuO-ZnO in the field of hydrogen (H_2) gas generation. For example, Liu et al. [83] showed the photocatalytic hydrogen production by the nanocomposite in the mixture of methanol and water. Hydrogen generation rate was 1700 μmol/h per g of CuO-ZnO catalyst, which is better than many other semiconductor oxide catalysts [90–93]. Simon et al. [18] showed the application of CuO-ZnO for photocatalytic hydrogen (production rate was 2 $\mu mol/h \cdot cm^2$ of the CuO-ZnO catalyst). Kargar et al. [50] also investigated the applicability of the nanocomposite for clean solar hydrogen generation at a large scale. The possible reason of better hydrogen production rate was due to the enlarged specific surface area, which provides more reaction sites, promote mass transfer, promote electron transfer from ZnO to CuO, reduce the recombination of electrons and holes, avoids photocorrosion of ZnO, and good sedimentation ability.

4.5 Humidity sensor

Baek and Tuller [16] prepared a CuO-ZnO heterojunction plate for the humidity sensor, which is very expensive. Further researchers have prepared several CuO-ZnO humidity sensors: Zainelabdin et al. [56] showed a sensitivity factor value of ~6045 for the CuO-ZnO nanocomposite, which is higher than its individual component [94–97]. Also, it showed a response and recovery time of 6 s and 7 s, respectively. Ashok et al. [53] used the CuO-ZnO nanocomposite as a humidity sensor, and the result shows better sensing properties with increasing temperature from 500°C to 600°C. Yoo et al. [96] and Qi et al. [97] also showed the application of the nanocomposite as a good humidity sensor. Also, with increasing temperature, the porosity of the nanocomposite increased, which enhanced the sensitivity value. An increase in the sensitivity is associated with a decrease in resistance or increases in electrical conduction, which is due to the attachment of cations of the heterojunction nanocomposite with the hydroxyl group of the adsorbed water.

4.6 Optoelectronic and magnetic storage devices

Vijayalakshmi and Karthick [51], Vijayakumar et al. [19], Udayabhaskar and Karthikeyan [42], and Gajendiran and Rajendran [13] showed that the CuO-ZnO nanocomposite has excellent optical and PL emission properties, which reveals its usability for optoelectronic devices. Better PL emission properties illustrated its better crystallinity and lesser intrinsic defect properties, which are excellent phenomena for optoelectronic devices. Optical transmittance is another important phenomenon for optoelectronic devices. Literature reveals that the transmittance of a nanocomposite (~86%) is higher than its individual component (~76%), which is due to the enhanced crystallinity and structural homogeneity of the nanocomposite. Incorporation of CuO within ZnO diminishes the scattering effect and point defect within ZnO.

Gajendiran and Rajendran [13], Zaoui et al. [12], and Buchholz and Chang [66], Chakrabarti et al. [98], and Tiwari et al. [31] studied its magnetic behavior, and the result revealed that the hysteresis loop exhibited room temperature ferromagnetic behavior and homogeneous distribution of the magnetic dopant. Intrinsically, nonmagnetic dopants were incorporated within the semiconductor to avoid the problem of magnetic precipitate, as the precipitate of these dopants do not precipitate in ferromagnetism. The literature shows that as Cu is a nonferromagnetic metal, thus, the composite made of Cu would show an intrinsic ferromagnetism property; although it is a controversial topic, further detailed studies need to be done for the magnetic device made of CuO-ZnO nanocomoposites.

4.7 Other applications

A few other important environmental applications of the CuO-ZnO nanocomposite has also been reported. For example, Zhou et al. [46] prepared porous CuO-ZnO hierarchical nanocomposite (HNC) nonenzymatic glucose electrodes as a glucose sensor. Liu et al. [70] showed that the nanocomposite had better antibacterial activity than its individual component due to the synergic effect of the nanocomposite.

All the CuO-ZnO nanocomposite synthesis techniques, material used, morphology, and their various applications are summarized and listed in Table 3.

5 Summary and outlook

Zn oxide, an n-type semiconductor with a band gap of 3.37 eV, has gained more attention in the field of nanoscience and technology because of its unique properties and potential applications. ZnO has been synthesized and modified by various techniques to improve its various properties, and the nanocomposite was made by doping

Table 3: Summary of CuO-ZnO nanocomposite synthesis technique, morphology, and its various applications.

Fabrication technique	Precursors/materials	Morphology and size	Applications	References
Co-precipitation	Zn chloride, Cu sulfate	Flowerlike ZnO adorned with leaf-like CuO	Photocatalytic activity	Li and Wang [17]
Co-precipitation	Cu(II) chloride, Zn sulfate	Flower-shaped ZnO along with leaf-shaped CuO	Photocatalytic activity	Das and Srivastava [37]
Co-precipitation	Zn acetate dehydrate, Cu acetate dehydrate	Spherical, 10–50 nm	Ferromagnetic behavior	Gajendiran and Rajendran [13]
Co-precipitation	Cu metal, ZnO, ammonium bicarbonate	Spherical, ~20 nm	Photocatalytic activity	Liu et al. [39]
Chemical vapor deposition	Bis(ketoiminato) Zn(II), Cu target	L ~400 nm	H_2 production	Simon et al. [18]
Sol-gel method	Zn acetate, Cu acetate	Cylindrical, d ~50–100 nm	Optic studies	Vijayakumar et al. [19]
Sol-gel, hydrothermal method	Zn acetate dihydrate and Cu acetate	Nanoflower, ~2 μm	Gas sensor	Haque et al. [40]
Sol-gel method	Zn acetate dehydrate, Cu acetate	Spherical, 5–60 nm	Gas sensor	Gomez-Pozos et al. [41]
Sol-gel method	Zn nitrate, Cu nitrate	Nanoflakes, ~100 nm	Optical study	Udayabhaskar and Karthikeyan [42]
Sol-gel method	Zn acetate dehydrate, Cu acetate	Flower shaped, ~21 nm	Ammonia gas sensor	Liu et al. [32]
Sol-gel method	Zn sulfate heptahydrate, Cu sulfate pentahydrate	–	Photocatalytic activity	Muzakki et al. [44]
Wet impregnation method	ZnO nanoparticle, Cu sulfate	Truncated octahedron, d ~50–70 nm, L ~few 100 nm	Photocatalytic activity	Sathishkumar et al. [20]
Thermal decomposition method	Zn acetate dehydrate, Cu acetate	Nanorod, d ~35 nm	Photocatalytic activity	Saravanan et al. [1]
Complex-directed hybridization	Zn acetate, Cu nitrate	3D micro-flowers 1–2 μm	Gas sensor, photocatalytic activity	Yang et al. [21]
Directly heating	Brass	Nanowires, L ~4–8 μm, d ~40–200 nm	Electronic devices	Zhu et al. [45]
Electrospinning	Zn acetate, Cu acetate	Truncated, d ~ 200 nm	Non-enzymatic glucose sensor	Zhou et al. [46]
Electrospinning	Zn nitrate and Cu acetate	Nanorod, ~100 nm	Photocatalytic activity	Ang et al. [47]
Electrospinning	Cu chloride, Zn acetate	Nanofibers, d ~100 nm, L ~several millimeters	H_2S sensing	Zhao et al. [22]
Electrospinning	Zn nitrate, Cu sulfate	Nanofilm	Solar cell	Jeong et al. [48]
Thermal oxidation	Cu and Zn Sheet	Nanowire, d ~30–100 nm, L ~5–20 μm	Electronic application	Zhao et al. [41]
Thermal oxidation	Cu foil, ZnO target	Nanowire, L ~4 μm	Solar hydrogen production	Kargar et al. [50]
Microwave synthesis	Zn acetate, Cu acetate	Flower shaped, ~200–300 nm	Optoelectronic devices	Vijayalakshmi and Karthick [51]
Microwave synthesis	Zn acetate dehydrate, Cu(II) nitrate	Nanorod d ~70 nm	Photocatalytic activity	Aliyu et al. [52]
Microwave synthesis	Zn acetate, Cu acetate	Agglomerated porous particle, ~34, ~46 nm	Humidity sensor	Ashok et al. [53]
Hydrothermal method	Zn acetate dehydrate, Cu nitrate-3-hydrate	Nanoflakes on hexagonal rods, d ~2 μm	Photoelectric behavior	Choudhary et al. [54]
Hydrothermal method	Zn chloride, Cu(II) acetate	Nanoplates, 300–500 nm	Photocatalytic activity	Chang et al. [55]
Hydrothermal method	Zn nitrate, Cu nitrate	Coral-like nanostructures on nanorods L ~1.5 μm, d ~80–120 nm	Humidity sensor	Zainelabudin et al. [56]
Hydrothermal method	Zn chloride, Cu nitrate	Flower shaped, ~100–200 nm	H_2S gas sensor	Kim et al. [57]
Hydrothermal method	Zn chloride, Cu chloride	Nano film	Gas sensor	Wang et al. [23]
Hydrothermal method	–	–	Electrochemical supercapacitor	Karunakaran and Manikandan [24]

Table 3 (continued)

Fabrication technique	Precursors/materials	Morphology and size	Applications	References
Hydrothermal method	Zn acetate, Cu wire	Nanorod, d ~50–200 nm, L ~6–10μm	H_2S sensing	Datta et al. [58]
Hydrothermal method, one-pot fabrication route	Zn acetate, Cu chloride	Hollow sphere, ~400 nm	Photocatalytic activity	Zhang et al. [59]
Hydrothermal method	–	Nnaorod, 100–400 nm	Photocatalytic activity	Ang et al. [47]
Cathodic electrodeposition	Zn chloride, Cu chloride	2D hexagonal sheets, thickness of ~0.5 mm	Electronic application	Sheini et al. [61]
Photo-deposition method	Metallic Zn, Cu nitrate	Thin film	Photocatalytic activity	Wang et al. [62]
Dielectric barrier discharge reactor	Brass mesh, brass foil, and Cu foil	Cluster shape, 200–300 nm	Gas sensor	Xia et al. [63]
Alkaline vapor oxidation process	Brass plate	Nanorod, d ~90 nm, L ~3 μm	Glucose oxidation	Soejima et al. [64]
Electrochemical method	Cu, Zn sheet, succinic acid	Spherical, 90–150 nm	Optoelectronic devices	Das and Srivastava [65]
Two-step solution process	Zn acetate dehydrate, Zn nitrate hexahydrate, Cu(II) nitrate trihydrate	Nanorod, d ~60 nm, L ~800 nm	Optoelectronic devices	Wang and Lin [11]
Pulsed-laser ablation	Zn target, Cu target	Thin film	Magnetic properties	Buchholz and Chang [66]
Solid state metathesis technique	Zn chloride, Cu chloride	Agglomerated nanoparticle, ~30 nm	Photocatalytic activity	Jacob et al. [67]
Magnetron sputtering	Cu sheets	Thin film	Solar cells	Minami et al. [68]
Electrodeposition method	Zn nitrate, Cu acetate	Nanorod, d ~200 nm L ~1 μm	Photocatalytic activity	Jiang et al. [69]
Solution-based process	Zn acetate, Cu nitrate	Nanorod, d ~50–100 nm, L ~3–4 mm	Photocatalytic activity	Jung and Yong [82]
Hydrothermal method	Zn acetate dehydrate, Cu sulfate pentahydrate	Nanorod, L ~10–20 μm, d ~1 μm	Photocatalytic activity	Liu et al. [84]
Chemical solution method	Zn nitrate hexahydrate, Cu nitrate trihydrate	Flower, ~10 μm	Gas sensor	Huang et al. [87]
Galvanostatic method	Cu(II) sulfate, Zn nitrate	Thin film	Solar cell	Kidowaki et al. [88]
Deposition method	Pure Cu	Nanowire with a Head, L ~2.1 μm, d ~70–100 nm,	Solar cells	Hsueh et al. [89]
Hydrothermal and photodeposition method	Zn acetate dehydrate, Cu sulfate pentahydrate	Corn-like stricture, d ~1–2 μm L ~10–20 μm	Hydrogen generation	Liu et al. [83]

with various nanomaterials like noble metals, metal oxide, and some complex oxides. Among all Cu-doped Zn oxide, the nanocomposites attained more attention because of its higher efficiency as a catalyst, sensor, solar cell, and optoelectronic device.

This article gives an overview of the Cu-doped ZnO nanocomposite synthesis and its various applications in the different practical fields. Various applications of the nanocomposite in the field of photocatalytic toxic dye degradation, optoelectronic and magnetic storage devices, gas sensor, solar cell, hydrogen generation, glucose sensor, and humidity sensor were also demonstrated. Taking advantage of the various facts such as an enlarge surface area due to the heterogeneous structure, which gives more reactive sites, promote mass transfer, promote electron transfer from ZnO to CuO, and avoid photocorrosion of nanocomposite shows its better performance than its individual component.

The improved knowledge on surface chemistry, methods of morphological modifications, and progress in the colloidal synthesis has helped in the CuO-ZnO nanocomposite preparation. The cooperative effects between CuO and ZnO have helped in exploring a variety of new applications ranging from the water treatment to the semiconductor applications. Despite the significant progress, challenges exist in the application on an industrial scale. CuO-ZnO-based materials have been used for various applications in the research stage; however, more research is required to extend their application range from a commercial point of view. Practical applications of the CuO-ZnO nanocomposites are limited and are considered as a future perspective only. High-end applications of

these nanocomposites will still require a lot of research to understand the interaction between the two oxides for applications in various fields: sensor, photocatalysis, semiconductor, and so on. Homogenous dispersion of one material into another requires a lot of further research. The properties of the CuO-ZnO nanocomposites are highly structure/size and ratio dependent. Still, further studies are required to provide better insights of the CuO-ZnO structure-property relationship. The important issues that need more attention are dispersion, size, porosity, rate of synthesis, and cost effectiveness. Overall, the processing-structure-property maps need to be developed. The engineering aspects of the CuO-ZnO nanocomposite manufacturing also need to be studied in detail. Also, performance indices may be developed vis-à-vis specified applications for composites made using different methods. Mass fabrication of the well-defined morphology of the CuO-ZnO nanocomposite with tunable function still remains to be a challenge for industrial purposes.

Acknowledgments: Dr. Das acknowledges the Science and Engineering Research Board, Department of Science and Technology, Government of India, for the financial support. Funder Name: DST-SERB-INDIA, Grant Number: SB/FTP/ETA-0121/2014.

References

[1] Saravanan R, Karthikeyan S, Gupta VK, Sekaran G, Narayanan V, Stephen A. Enhanced photocatalytic activity of ZnO/CuO nanocomposite for the degradation of textile dye on visible light illumination. *Mater. Sci. Eng. C* 2013, 33, 91–98.

[2] Bandara J, Pradeep UW, Bandara RGSJ. The role of n–p junction electrodes in minimizing the charge recombination and enhancement of photocurrent and photovoltage in dye sensitized solar cells. *J. Photochem. Photobiol. A Chem*. 2005, 170, 273–278.

[3] Anicai L, Petica A, Patroi D, Marinescu V, Prioteasa P, Costovici S. Electrochemical synthesis of nanosized TiO_2 nanopowder involving choline chloride based ionic liquids. *Mater. Sci. Eng. B* 2015, 199, 87–95.

[4] Mariammal RN, Ramachandran K, Renganathan B, Sastikumar D. On the enhancement of ethanol sensing by CuO modified SnO_2 nanoparticles using fiber-optic sensor. *Sens. Actuators B* 2012, 169, 199–207.

[5] Yang H, Tao Q, Zhang X, Tang A, Ouyang J. Solid-state synthesis and electrochemical property of SnO_2/NiO nanomaterials. *J. Alloy Compd*. 2008, 459, 98–102.

[6] Fang J, Ma J, Sun Y, Liu Z, Gao C, Electrochemical synthesis of nanocrystalline $SrNb_2O_6$ powders and characterization of their photocatalytic property. *Mater. Sci. Eng. B* 2011, 176, 701–705.

[7] Jin Z, Zhang X, Li Y, Li S, Lu G. 5.1% Apparent quantum efficiency for stable hydrogen generation over eosin-sensitized CuO/TiO_2 photocatalyst under visible light irradiation. *Catal. Commun*. 2007, 8, 1267–1273.

[8] Li B, Hao Y, Zhang B, Shao X, Hub L. A multifunctional noble-metal-free catalyst of CuO/TiO2 hybrid nanofibers. *Appl. Catal A: Gen*. 2017, 531, 1–12.

[9] Jun ST, Choi GM. Composition dependence of the electrical conductivity of ZnO(n)–CuO(p) ceramic composite. *J. Am. Ceram. Soc*. 1998, 81, 695–699.

[10] Zhang D. Synthesis and characterization of ZnO-doped cupric oxides and evaluation of their photocatalytic performance under visible light. *Transit. Met. Chem*. 2010, 35, 689–694.

[11] Wang RC, Lin HY. ZnO-CuO core-shell nanorods and CuO-nanoparticle-ZnO-nanorod integrated structures. *Appl. Phys. A* 2009, 95, 813–818.

[12] Zaoui A, Ferhat M, Ahuja R. Magnetic properties of (ZnO)1/(CuO)1(001) superlattice. *Appl. Phys. Lett*. 2009, 94, 102102.

[13] Gajendiran J, Rajendran V. Synthesis and characterization of coupled semiconductor metal oxide (ZnO/CuO) nanocomposite. *Mater. Lett*. 2014, 116, 311–313.

[14] Nakamura Y, Yoshioka N, Miyayama M, Yanagida H, Tsurutani T, Nakamura Y. Selective CO gas sensing mechanism with CuO. ZnO heterocontact. *J. Electrochem. Soc*. 1990, 137, 940–943.

[15] Ushio Y, Miyayama M, Yanagida H. Effects of interface states on gas-sensing properties of a CuO/ZnO thin-film heterojunction. *Sens. Actuators B* 1994, 17, 221–226.

[16] Baek KK, Tuller HL. Atmosphere sensitive CuO/ZnO junctions. *Solid State Ionics* 1995, 75, 179–186.

[17] Li B, Wang Y. Facile synthesis and photocatalytic activity of ZnO-CuO Nanocomposite. *Superlattices Microstruct*. 2010, 47, 615–623.

[18] Simon Q, Barreca D, Gasparotto A, Maccato C, Montini T, Gombac V, Fornasiero P, Lebedev O, Turnere S, Tendeloo GV. Vertically oriented CuO/ZnO nanorod arrays: from plasma-assisted synthesis to photocatalytic H_2 production. *J. Mater. Chem*. 2012, 22, 11739–11747.

[19] Vijayakumar GNS, Devashanka S, Rathnakumari M, Sureshkumar P. Synthesis of electrospun ZnO/CuO nanocomposite fibers and their dielectric and non-linear optic studies. *J. Alloys Compd*. 2010, 507, 225–229.

[20] Sathishkumar P, Sweena R, Wu JJ, Anandan S. Synthesis of CuO-ZnO nanophotocatalyst for visible light assisted degradation of a textile dye in aqueous solution. *Chem. Eng. J*. 2011, 171, 136–140.

[21] Yang C, Cao X, Wang S, Zhang L, Xiao F, Su X, Wang J. Complex-directed hybridization of CuO/ZnO nanostructures and their gas sensing and photocatalytic properties. *Ceram. Int*. 2015, 41, 1749–1756.

[22] Zhao M, Wang X, Ning L, Jia J, Li X, Cao L. Electrospun Cu-doped ZnO nanofibers for H_2S sensing. *Sens. Actuators B* 2011, 156, 588–592.

[23] Wang JX, Sun XW, Yang Y, AKyaw KK, Huang XY, Yin JZ, Wei J, Demir HV. 4 Free-standing ZnO-CuO composite nanowire array films and their gas sensing properties. *Nanotechnology* 2011, 22, 325704.

[24] Karunakaran C, Manikandan G. Synthesis and characterization of Zn-doped CuO nanomaterials for electrochemical supercapacitor applications. *National Conference on Recent Advances in Surface Science* 2013, 93–95.

[25] Harisha S, Archana J, Sabarinathana M, Navaneethana M, Nisha KD, Ponnusamy S, Muthamizhchelvan C, Ikeda H, Aswal DK,

Hayakawa Y. Controlled structural and compositional characteristic of visible light active ZnO/CuO photocatalyst for the degradation of organic pollutant. *Appl. Surf. Sci*. 418, 2017, 103–112.
[26] Thakur VK, Kessler MR. Self-healing polymer nanocomposite materials: a review. *Polymer* 2015, 69, 369–383.
[27] Puggal S, Dhall N, Singh N, Litt MS. A review on polymer nanocomposites: synthesis, characterization and mechanical properties. *Ind. J. Sci. Technol*. 2016, 9, 1–6.
[28] Gao N, Fang X. Synthesis and development of graphene–inorganic semiconductor nanocomposites. *Chem. Rev*. 2015, 115, 8294–8343.
[29] Raman N, Sudharsan S, Pothiraj K. Synthesis and structural reactivity of inorganic–organic hybrid nanocomposites – a review. *J. Saudi Chem. Soc*. 2012, 16, 339–352.
[30] Camargo PHC, Satyanarayana KG, Wypych F. Nanocomposites: synthesis, structure, properties and new application opportunities. *Mater. Res*. 2009, 12, 1–39.
[31] Tiwari A, Snure M, Kumar D, Abiade JT. Ferromagnetism in Cu-doped ZnO films: role of charge carriers. *Appl. Phys. Lett*. 2008, 92, 062509.
[32] Liu HL, Yang JH, Hua Z, Zhang YJ, Yang LL, Xiao L, Xie Z. The structure and magnetic properties of Cu-doped ZnO prepared by sol–gel method. *Appl. Surf. Sci*. 2010, 256, 4162–4165.
[33] Wu JJ, Liu SC. Catalyst-free growth and characterization of ZnO nanorods. *J. Phys. Chem. B*. 2002, 106, 9546–9551.
[34] Zhao J, Yan XQ, Yang Y, Huang YH, Zhang Y. Raman spectra and photoluminescence properties of In-doped ZnO nanostructures. *Mater. Lett*. 2010, 64, 569–572.
[35] Takata M, Tsubone D, Yanagida H. Dependence of electrical-conductivity of ZnO on degree of sensing. *J. Am. Ceram. Soc*. 1976, 59, 4–8.
[36] Huang D, Zhao Y, Chen D, Shao YZ. Magnetism and clustering in Cu doped ZnO. *Appl. Phys. Lett*. 2008, 92, 182509.
[37] Das S, Srivastava VC. Hierarchical nanostructured ZnO-CuO nanocomposite and its photocatalytic activity. *J. Nano. Res*. 2016, 35, 21–26.
[38] Bagabas A, Aboud MFA, Mohamed RM, AL-Othman Z, Alshammari AS, Addurihem ES. Synthesis, characterization, and cyanide photodegradation over cupric oxide-doped zinc oxide nanoparticles. *ACS Symposium Series* 2013, 1124, 327–338.
[39] Liu ZL, Deng JC, Deng JJ, Li FF. Fabrication and photocatalysis of CuO/ZnO nano-composites via a new method. *Mater. Sci. Eng. B* 2008, 150, 99–104.
[40] Haque FZ, Singh N, Ranjan P. Synthesis of ZnO/CuO nanocomposite and optical study of ammonia (NH_3) gas sensing. *Int. J. Sci. Eng. Res*. 2014, 5, 149–151.
[41] Gomez-Pozos H, Arredondo EL, Álvarez AM, Biswal R, Kudriavtsev Y, Vega Pérez J, Casallas-Moreno YL, Amador MLO. Cu-doped ZnO thin films deposited by a sol-gel process using two copper precursors: gas-sensing performance in a propane atmosphere. *Materials* 2016, 87, 1–16.
[42] Udayabhaskar R, Karthikeyan B. Optical and phonon properties of ZnO:CuO mixed nanocomposite. *J. Appl. Phys*. 2014, 115, 154303.
[43] Liu C, Liu Z, Li J, Li Y, Han J, Wang Y, Liu Z, Ya J. Cu-doping ZnO/ZnS nanorods serve as the photoanode to enhance photocurrent and conversion efficiency. *Microelectron. Eng*. 2013, 103, 12–16.
[44] Muzakki A, Shabrany H, Saleh R. Synthesis of ZnO/CuO and TiO_2/CuO nanocomposites for light and ultrasound assisted degradation of a textile dye in aqueous solution, In *3rd International Conference on Advanced Materials Science and Technology*. ICAMST, 2015.
[45] Zhu BY, Sow CH, Yu T, Zhao Q, Li P, Shen Z, Yu D, Thong JTL. Co-synthesis of ZnO-CuO nanostructures by directly heating brass in air. *Adv. Funct. Mater*. 2016, 16, 2415–2422.
[46] Zhou C, Xu L, Song J, Xing R, Xu S, Liu D, Song H. Ultrasensitive non-enzymatic glucose sensor based on three-dimensional network of ZnO-CuO hierarchical nanocomposites by electrospinning. *Sci. Report* 2014, 4, 1–9.
[47] Ang W, Li X, Li S, Yan-Jun L, Wei-Wei L. CuO nanoparticle modified ZnO nanorods with improved photocatalytic activity. *Chin. Phys. Lett*. 2013, 30, 046202.
[48] Jeong SS, Mittiga A, Salza E, Masci A, Passerini S. Electrodeposited ZnO/Cu_2O heterojunction solar cells. *Electrochim. Acta* 2008, 53, 2226–2231.
[49] Zhao J, Zhang C, Wang D. A facile one-step synthesis of p-CuO/n-ZnO nanowire heterojunctions by thermal oxidation route. *Mater. Sci. Semicond. Process*. 2015, 35, 55–58.
[50] Kargar A, Jing Y, Joo Kim S, Riley CT, Pan X, Wang D. ZnO/CuO heterojunction branched nanowires for photoelectrochemical hydrogen generation. *ACS Nano* 2013, 7, 11112–11120.
[51] Vijayalakshmi K, Karthick K. High quality ZnO/CuO nanocomposites synthesized by microwave assisted reaction. *J. Mater. Sci. Mater. Electron*. 2014, 25, 832–836.
[52] Aliyu SH, Abdullah HA, Abbas Z. Solid state characterization of Cu-ZnO nanocomposite synthesised via micro-wave irradiation. *Int. J. Eng. Sci*. 2014, 3, 47–53.
[53] Ashok CH, Rao KV, Chakra CHS. Facile synthesis and characterization of ZnO/CuO nanocomposite for humidity sensor application. *J. Adv. Chem. Sci*. 2016, 2, 223–226.
[54] Choudhary MA, Ahmad Z, Hassan A, Khan Y, Aslam M. Synthesis and characterization of ZnO/CuO nanocomposites on porous 3d ni substrate and its photoelectric behavior. *Synth. React. Inorg. M* 2016, 46, 1618–1621.
[55] Chang T, Li Z, Yun G, Jia Y, Yang H. Enhanced photocatalytic activity of ZnO/CuO nanocomposites synthesized by hydrothermal method. *Nano-Micro Lett*. 2013, 5, 163–168.
[56] Zainelabdin A, Amin G, Zaman S, Nur O, Lu J, Hultman L, Willande M. CuO/ZnO Nanocorals synthesis via hydrothermal technique: growth mechanism and their application as humidity sensor. *J. Mater. Chem*. 2012, 22, 11583–11590.
[57] Kim J, Kim W, Yong K. CuO/ZnO heterostructured nanorods: photochemical synthesis and the mechanism of H_2S gas sensing. *J. Phys. Chem. C* 2012, 116, 15682–15691.
[58] Datta N, Ramgir NS, Kumar S, Veerender P, Kaur M, Kailasaganapathi S, Debnath AK, Aswal DK, Gupta SK. Role of various interfaces of CuO/ZnO random nanowire networks in H_2S sensing: An impedance and Kelvin probe analysis. *Sens. Actuators B* 2014, 202, 1270–1280.
[59] Zhang C, Yin L, Zhang L, Qi Y, Lun N. Preparation and photocatalytic activity of hollow ZnO and ZnO-CuO composite spheres. *Mater. Lett*. 2012, 67, 303–307.
[60] Xu Z, Duan G, Li Y, Liu G, Zhang H, Dai Z, Cai W. CuO-ZnO micro/nanoporous array-film-based chemosensors: new sensing properties to H_2S. *Chem. Eur. J*. 2014, 20, 6040–6046.
[61] Sheini FJ, Singh J, Srivasatva ON, Joag DS, More MA. Electrochemical synthesis of Cu/ZnO nanocomposite films and their efficient field emission behavior. *Appl. Surf. Sci*. 2010, 256, 2110–2114.

[62] Wang J, Fan XM, Wu DZ, Dai J, Liu H, Liu HR, Zhou ZW. Fabrication of CuO/T-ZnOw nanocomposites using photodeposition and their photocatalytic property. *Appl. Surf. Sci*. 2011, 258, 797–1805.
[63] Xia H, Zhou R, Zheng C, Wu P, Tian Y, Hou X. Solution-free, in situ preparation of nano/micro CuO/ZnO in dielectric barrier discharge for sensitive cataluminescence sensing of acetic acid. *Analyst* 2013, 138, 3687–3691.
[64] Soejima T, Takad K, Ito S. Alkaline vapor oxidation synthesis and electrocatalytic activity toward glucose oxidation of CuO/ZnO composite nanoarrays. *Appl. Surf. Sci*. 2013, 277, 192–200.
[65] Das S, Srivastava VC. Synthesis and characterization of ZnO/CuO nanocomposite by electrochemical method. *Mater. Sci. Semicond. Process*. 2017, 57, 173–177.
[66] Buchholz DB, Chang RPH. Room-temperature ferromagnetism in Cu-doped ZnO thin films. *Appl. Phys. Lett*. 2005, 87, 082504.
[67] Jacob NM, Madras G, Kottkamp N, Thomas T. Multivalent Cu-doped ZnO nanoparticles with full solar spectrum absorbance and enhanced photoactivity. *Ind. Eng. Chem. Res*. 2014, 53, 5895–5904.
[68] Minami T, Miyata T, Ihara K, Minamino Y, Tsukada S. Effect of ZnO film deposition methods on the photovoltaic properties of ZnO-Cu_2O heterojunction devices. *Thin Solid Films* 2006, 494, 47–52.
[69] Jiang X, Zhang M, He G, Sun Z. Microstructure, optical properties, and catalytic performance of Cu_2O-modified ZnO nanorods prepared by electrodeposition. *Nanoscale Res. Lett*. 2015, 10, 30.
[70] Fernandes DM, Silva R, Winkler Hechenleitner AA, Radovanovic E, Custodio Melo MA, Gomez Pineda EA. Synthesis and characterization of ZnO, CuO and a mixed Zn and Cu oxide. *Mater. Chem. Phys*. 2009, 115, 110–115.
[71] Maddahi P, Shahtahmasebi N, Kompany A, Mashreghi M, Safaee S, Roozban F. Effect of doping on structural and optical properties of ZnO nanoparticles: study of antibacterial properties. *Mater. Sci. Poland* 2014, 32, 130–135.
[72] Apaydin F, Ozkan Toplan H, Yildiz K. The effect of CuO on the grain growth of ZnO. *J. Mater. Sci*. 2005, 40, 677–682.
[73] Sahar MDR, Budi AS. Optical band gap and IR spectra of glasses in the system [Nd_2O_3](x)- [CuO](35-x)-[P_2O_5](65). *J. Solid State Sci. Technol*. 2006, 14, 115–120.
[74] Sonawane BK, Bhole MP, Patil DS. Effect of magnesium incorporation in zinc oxide films for optical waveguide applications. *Physica B: Condense Matter* 2010, 405, 1603–1607.
[75] Chen H, Ding J, Ma SH, Structural and optical properties of ZnO:Mg thin films grown under different oxygen partial pressures. *Physica E: Low-Dimensional Systems and Nanostructures* 2010, 42, 1487–1491.
[76] Yan Y, Al-Jassim MM, Wei S. Doping of ZnO by group-IB elements. *Appl. Phys. Lett*. 2006, 89, 181912.
[77] Viswanatha R, Chakraborty S, Basu S, Sarma DD. Blue-emitting copper-doped zinc oxide nanocrystals. *J. Phys. Chem. B* 2006, 110, 22310–22312.
[78] Ma Q, Buchholz DB, Chang RPH. Local structures of copper-doped ZnO films. *Phys. Rev. B* 2008, 78, 214429.
[79] Steiner, Kinsinger P, Sander V, Siegwart I, Hufner B, Politis SC, Hoppe CR, Muller HP. The Cu valence in the high Tc superconductors and in monovalent, divalent and trivalent copper oxides determined from XPS core level spectroscopy. *J. Phys. B. Condensed Matter* 1987, 67, 497 – 502.
[80] Hoa ND, Van Quy N, Jung H, Kim D, Kim H, Hong SK. Synthesis of porous CuO nanowires and its application to hydrogen detection. *Sens. Actuators B* 2010, 146, 266–272.
[81] Ashcroft NW, Mermin ND. *Solid State Physics*. Harcourt: Fort Worth, Texas, 1975.
[82] Jung S, Yong K. Fabrication of CuO-ZnO nanowires on a stainless steel mesh for highly efficient photocatalytic applications. *Chem. Commun*. 2011, 47, 2643–2645.
[83] Liu Z, Bai H, Xu S, Sun DD. Hierarchical CuO/ZnO "corn-like" architecture for photocatalytic hydrogen generation. *Int. J. Hydrog. Energy* 2011, 36, 13473–13480.
[84] Liu Z, Bai H, Sun DD. Hierarchical CuO/ZnO membranes for environmental, applications under the irradiation of visible light. *Int. J. Photoenergy* 2011, 2012, 1–11.
[85] Hassan JJ, Mahdi MA, Chin CW, Abu-Hassan H, Hassan Z. Room temperature hydrogen gas sensor based on ZnO nanorod arrays grown on a SiO_2/Si substrate via a microwave-assisted chemical solution method. *J. Alloys Compd*. 2013, 546, 107–111.
[86] Ma X, Song H, Guan C. Interfacial oxidation–dehydration induced formation of porous SnO_2 hollow nanospheres and their gas sensing properties. *Sens. Actuators B* 2013, 177, 196–204.
[87] Huang J, Dai Y, Gu C, Sun Y, Liu J. Preparation of porous flower-like CuO/ZnO nanostructures and analysis of their gas-sensing property. *J. Alloys Compd*. 2013, 575, 115–122.
[88] Kidowaki H, Oku T, Akiyama T. Fabrication and characterization of CuO/ZnO solar cells. *J. Phys: Conference Series* 2012, 352, 012022.
[89] Hsueh TJ, Hsu CL, Chang SJ, Guo PW, Hsieh JHH, Chend IC. Cu_2O/n-ZnO nanowire solar cells on ZnO:Ga/glass templates. *Scr. Mater*. 2007, 57, 53–56.
[90] Kudo A, Miseki Y. Heterogeneous photocatalyst materials for water splitting. *Chem. Soc. Rev*. 2009, 38, 253–278.
[91] Kudo A. Development of photocatalyst materials for water splitting. *Int. J. Hydrog. Energy* 2006, 31, 197–202.
[92] Zhou H, Li X, Fan T, Osterloh FE, Ding J, Sabio EM. Artificial inorganic leafs for efficient photochemical hydrogen production inspired by natural photosynthesis. *Adv. Mater*. 2010, 22, 951–956.
[93] Wu NL, Lee MS. Enhanced TiO_2 photocatalysis by Cu in hydrogen production from aqueous methanol solution. *Int. J. Hydrog. Energy* 2004, 29, 1601–1605.
[94] Zhang Y, Yu K, Jiang D, Geng H, Luo L. Zinc oxide nanorod and nanowire for humidity sensor. *Appl. Surf. Sci*. 2005, 24, 212–217.
[95] Xu J, Yu K, Wu J, Shang D, Li L, Xu Y, Zhu Z. Synthesis, field emission and humidity sensing characteristics of honeycomb-like CuO. *J. Phys. D Appl. Phys*. 2009, 42, 075417.
[96] Yoo DJ, Park SJ. Electrolysis of water in CuO/ZnO heterocontact humidity sensor. *J Electrochem. Soc*. 1996, 143, L89–L91.
[97] Qi Q, Zhang T, Zeng Y, Yang H. Humidity sensing properties of KCl-doped Cu–Zn/CuO-ZnO nanoparticles. *Sens. Actuators B* 2009, 137, 21–26.
[98] Chakrabarti D, Narayan J. Room temperature ferromagnetism in thin films. *Appl. Phys. Lett*. 2007, 90, 062504.

Bionotes

Susmita Das
Department of Chemical Engineering,
Indian Institute of Technology Roorkee,
Roorkee-247667, India
susmita.82.das@gmail.com

Susmita Das received her PhD in Chemical Engineering from the Indian Institute of Technology (IIT) Kanpur in 2013. After a post-doctorate position at IIT Roorkee in 2014–2015, she joined the Department of Chemical Engineering, IIT Roorkee, as a Young Scientist Fellow. During her PhD, she worked on bioinspired fracture mechanics, and her current research interests include environmental science (specifically waste water treatment), catalysis, and nanoparticle synthesis and characterization.

Vimal Chandra Srivastava
Department of Chemical Engineering,
Indian Institute of Technology Roorkee,
Roorkee-247667, India
vimalcsr@yahoo.co.in; vimalfch@iitr.ac.in
http://orcid.org/0000-0001-5321-7981

Vimal Chandra Srivastava is an Associate Professor in the Department of Chemical Engineering, IIT Roorkee, India. His major research interests are industrial pollution abatement, desulfurization, catalysis, nanoparticle synthesis, CO_2 utilization, alternative fuels, etc. He has authored >145 papers, five book chapters and has received 6000 citations of his papers with an h-index of 34. He has guided 11 PhD and 45 M.Tech. students. He was awarded the Prosper.Net-SCOPUS Young Researcher Award 2010 – First Runner-up Prize, INAE Young Engineer Award 2012, INSA Young Scientist Medal 2012, IE Young Engineer Award 2013, and IIChE-Amar Dye-Chem Award 2013.